doi:10.1093/brain/awu078 Brain 2014: 137; 1716–1732 | 1716

BRAIN
A JOURNAL OF NEUROLOGY

Chasing central nervous system plasticity: the brainstem's contribution to locomotor recovery in rats with spinal cord injury

Björn Zörner,[1,*] Lukas C. Bachmann,[2,*] Linard Filli,[1] Sandra Kapitza,[1] Miriam Gullo,[2] Marc Bolliger,[3] Michelle L. Starkey,[3] Martina Röthlisberger,[2] Roman R. Gonzenbach[1] and Martin E. Schwab[2]

1 Department of Neurology, University Hospital Zurich, Frauenklinikstrasse 26, 8091 Zurich, Switzerland
2 Brain Research Institute, University of Zurich and Department of Health Sciences and Technology, ETH Zurich, Winterthurerstrasse 190, 8057 Zurich, Switzerland
3 Spinal Cord Injury Centre, Balgrist University Hospital, Forchstrasse 340, 8008 Zurich, Switzerland

*These authors contributed equally to this work.

Correspondence to: Dr med. Björn Zörner,
Department of Neurology, University Hospital Zurich,
Frauenklinikstr. 26, 8091 Zurich,
Switzerland
E-mail: bjoern.zoerner@usz.ch

Anatomical plasticity such as fibre growth and the formation of new connections in the cortex and spinal cord is one known mechanism mediating functional recovery after damage to the central nervous system. Little is known about anatomical plasticity in the brainstem, which contains key locomotor regions. We compared changes of the spinal projection pattern of the major descending systems following a cervical unilateral spinal cord hemisection in adult rats. As in humans (Brown-Séquard syndrome), this type of injury resulted in a permanent loss of fine motor control of the ipsilesional fore- and hindlimb, but for basic locomotor functions substantial recovery was observed. Antero- and retrograde tracings revealed spontaneous changes in spinal projections originating from the reticular formation, in particular from the contralesional gigantocellular reticular nucleus: more reticulospinal fibres from the intact hemicord crossed the spinal midline at cervical and lumbar levels. The intact-side rubrospinal tract showed a statistically not significant tendency towards an increased number of midline crossings after injury. In contrast, the corticospinal and the vestibulospinal tract, as well as serotonergic projections, showed little or no side-switching in this lesion paradigm. Spinal adaptations were accompanied by modifications at higher levels of control including side-switching of the input to the gigantocellular reticular nuclei from the mesencephalic locomotor region. Electrolytic microlesioning of one or both gigantocellular reticular nuclei in behaviourally recovered rats led to the reappearance of the impairments observed acutely after the initial injury showing that anatomical plasticity in defined brainstem motor networks contributes significantly to functional recovery after injury of the central nervous system.

Keywords: plasticity; brainstem; spinal cord injury; functional recovery

Abbreviation: MLR = mesencephalic locomotor region

Received November 3, 2013. Revised January 21, 2014. Accepted February 16, 2014. Advance Access publication April 15, 2014

Introduction

After injury to the CNS, varying degrees of functional recovery are observed depending typically on the location and size of the lesion. Identification of the underlying mechanisms of spontaneous recovery and the factors that impede further functional improvements is an important prerequisite for the development of effective new therapies for brain and spinal cord injury (Raineteau and Schwab, 2001; Courtine *et al*., 2011; Rossignol and Frigon, 2011). Anatomical plasticity in the CNS ranging from sprouting of lesioned and unlesioned fibres to the *de novo* formation of detour pathways has been shown to mediate functional recovery after brain and spinal cord injury in rodents and primates (Bareyre *et al*., 2004; Dancause *et al*., 2005; Courtine *et al*., 2008; Zorner and Schwab, 2010). After one-sided spinal cord injury (e.g. Brown-Séquard syndrome), spared contralateral tracts are believed to mediate functional recovery through pre-existing or newly formed fibres that cross the spinal cord midline below the level of the injury (Ghosh *et al*., 2009). Thus far, beneficial, spontaneous neuroanatomical adaptations are almost exclusively described in the sensorimotor cortex and its projections as well as in intraspinal networks (Nudo, 2006; Courtine *et al*., 2008). Much less is known about adjustments in other brain regions after CNS damage, in particular in the brainstem, which contains the phylogenetically oldest and functionally most important centres for basic movement control.

Key structures for the initiation and execution of locomotion are located in the midbrain, pons and medulla oblongata (Shik *et al*., 1969; Grillner, 1996). From fish to mammals, locomotor command regions located in the rostral brainstem such as the mesencephalic locomotor region (MLR) are directly connected to bulbar output systems, for example the medial reticular formation (Garcia-Rill *et al*., 1986; Webster and Steeves, 1991; Matsuyama *et al*., 2004; Ryczko and Dubuc, 2013). The reticular formation, in turn, projects to the spinal cord to initiate and coordinate limb movements and postural support, and to modulate the locomotor rhythm produced by the spinal central pattern generators (Grillner and Wallen, 1985; Matsuyama *et al*., 2004; Grillner *et al*., 2008; McCrea and Rybak, 2008). The rubrospinal system is involved in the execution of precise limb movements whereas vestibulospinal tracts primarily control balance and posture (Markham, 1987; Armstrong, 1988; Whishaw *et al*., 1998). Despite the fact that these phylogenetically highly conserved brainstem centres are crucial components of the CNS motor network, only limited information is currently available on their responses to CNS damage (Raineteau *et al*., 2001; Ballermann and Fouad, 2006; Courtine *et al*., 2008; Weishaupt *et al*., 2013). In particular, a comparative analysis of neuroanatomical changes in the different central nervous systems after injury is missing.

In this study, we assessed the anatomical plasticity in the major descending central nervous systems after cervical unilateral spinal cord hemisections in adult rats. We investigated whether changes in the spinal projection pattern of a plastic region are accompanied by anatomical remodelling of its input from other CNS centres and we evaluated the functional significance of these adaptations.

Materials and methods

Animals

Adult female Lewis rats, 10 weeks of age (200–250 g, R. Janvier, France) were housed in groups of three to five rats in standardized cages (type 4 Macrolon) under a 12-h light/dark cycle with food and water provided *ad libitum*. All experiments were approved by the Veterinary Office of the Canton of Zurich, Switzerland.

Spinal cord injury and animal care

Rats were deeply anaesthetized with subcutaneous injections of Hypnorm/Dormicum (Hypnorm: 120 µl/200 g body weight, Janssen Pharmaceutics; Dormicum 0.75 mg/200 g body weight, Roche Pharmaceuticals) for all surgical procedures described below. For cervical hemisection injury at C4 spinal level, the rats' skin was cut between the occipital bone and the prominent process of the T2 vertebra with a scalpel. Laminectomy of the third cervical vertebra was performed and the dura was opened along the rostrocaudal axis with a fine needle to expose the entire dorsal surface of the spinal cord. A 27-gauge needle was lowered at the spinal cord midline and served as boundary for the hemisection. As we found no paw preference in the cylinder test in this rat strain (see 'Results' section), all rats received a right-sided unilateral hemisection injury at cervical level C4. The right spinal hemicord was cut with a sharp sapphire knife (WPI). To ensure completeness of the lesion, cuts were repeated until the ventral surface of the spinal canal was visible. Following the lesion, the muscle layers were sutured and the skin was closed with surgical staples. One day before and for 2 days after surgery, rats received subcutaneous injections of the analgesic Rimadyl (5 mg/kg, Pfizer). To prevent bladder and wound infections, rats were treated with daily subcutaneous injections of the antibiotic Baytril (5 mg/kg body weight, Bayer) for 1 week. All rats were checked twice daily for the entire period of the experiment.

To assess a possible role of the myelin-associated neurite growth inhibitor Nogo-A, all chronic spinal cord injured animals received a 2-week intrathecal, thoracic spinal infusion of antibodies [control-IgG or anti-Nogo-A (11C7) antibodies; total amount infused: 6 mg] by way of an osmotic mini-pump (5 µl/h, 3.1 µg IgG/µl, Alzet 2ML2; Charles River Laboratories) starting at the time of injury. As shown by densitometry of immunostained sections on different levels of the spinal cord rostral to the lesion, antibodies did not efficiently diffuse into the spinal and brain parenchyma, most probably due to a continuous, lesion-induced dura leak at the cervical hemisection site during the time of infusion (data not shown). The subdural spaces were collapsed all along the spinal cord, supporting the hypothesis of a long-lasting, major CSF leak in this lesion paradigm. Clinically, large dura mater lesions are known to heal slowly (Sayad and Harvey, 1923). Because of the unavailability of the antibody in the tissue, antibody-treatment was disregarded. When control-IgG and anti-Nogo-A antibody treated animals were compared, no differences could be observed for any of the read-outs shown in the present study.

Perfusion and Nissl staining

After completion of the experiments, rats were anaesthetized with an overdose of pentobarbital (intraperitoneal) and transcardially perfused with 100 ml heparinized Ringer's solution followed by 400 ml Ringer's solution containing 4% paraformaldehyde and 5% sucrose. Brains and

spinal cords were removed, post-fixed in the same fixative overnight at 4°C, cryoprotected in 30% sucrose for 5 days, embedded in Tissue-Tek® and frozen in isopentane at −40°C. The tissue was cut on a cryostat and 40-µm thick cross-sections were collected on-slide. Completeness of hemisections was confirmed histologically on Nissl stained spinal cord cross-sections of the lesion centre. For staining, dried sections were bathed in Cresyl violet solution for 3 min, dehydrated in ethanol, washed in xylol and coverslipped with Eukitt® (Kapitza *et al*., 2012). Rats with incomplete hemisections were removed from analysis.

Behavioural testing and quantification

Rats were familiarized with the behaviour set-ups and trained on the tasks for a total of 5–7 sessions within 14 days. Baseline measurements were performed 1 week before spinal cord injury. To characterize the course of functional recovery after hemisection injury ($n = 20$; five rats were excluded retrospectively due to an incomplete hemisection), rats were tested 1, 2, 4, 8 and 12 weeks after lesion. Grooming behaviour was first assessed 2 weeks after injury and paw preference was tested only once, 1 week before hemisection.

The 'paw preference test' ('cylinder test') was performed to detect asymmetries in forelimb use for each individual rat before injury and evaluated according to earlier studies (Gensel *et al*., 2006). Also, air-righting was assessed and scored as published previously (Laouris *et al*., 1990; Pellis *et al*., 1991). In brief, rats were held in supine position ~30 cm above a surface covered with foam material. After being released intact rats land on their paws due to a successive rotation of head, shoulder girdle, thorax and pelvis. Air-righting reaction was tested 10 times per time point and video recorded. Scoring was performed based on the posture of the rat at landing (Laouris *et al*., 1990): 0 = no rotation, 1 = head rotation only, 2 = head and thorax rotation only, 3 = landing on the side, 4 = full rotation except hindlimbs, 5 = full rotation. Values represent the mean of 10 trials per rat. Grooming was assessed immediately after the swimming test (with wet fur) in a transparent Plexiglas cage filled with bedding. Grooming activity was recorded with a video camera for 3 min. Each forelimb was evaluated separately. Scoring was performed according to a previously published rating scheme (Bertelli and Mira, 1993; Gensel *et al*., 2006) based on the most remote part of the head that could be reached by the forepaws: 0 = no contact with the head, 1 = contact with snout (underneath), 2 = contact with the dorsal surface of the snout, 3 = contact with the area between eyes and the front of the ears (forehead), 4 = contact with the ears (front), 5 = contact with the area behind the ears. Over-ground walking, wading through 3-cm deep water, swimming and walking over a horizontal ladder was tested in a behavioural testing set-up ('MotoRater') described previously (Zorner *et al*., 2010). Before testing, the rats' skin overlying bony anatomical landmarks on fore- and hindlimbs was tattooed with a commercially available tattooing kit (Hugo Sachs Elektronik, Harvard Apparatus) to ensure reliable measurements over time. Locomotor behaviour was filmed with a high-speed video camera (Basler A504kc Color Camera) at 200 Hz and analysed with the ClickJoint software (version 5.0; ALEA Solutions). Parameters assessed during over-ground walking and wading were defined as follows: shoulder and hip height as the vertical distance between the joint and the runway; pro- and retraction of the fore- and hindlimbs as the maximal horizontal distance (forwards and backwards) between the wrist and the shoulder joint or between the toe (MTP) and the hip, respectively; paw dragging was present if toes touched the ground during the swing phase; the paw rotation angle ('external rotation') was defined as the angle between the body axis and the paw axis (line between the third MTP and the heel) and assessed at mid-stance; step width ('base of support') was calculated by adding the distances measured between the body axis and the left and the right heel for two consecutive (left-right) steps. Precise paw placement of fore- and hindlimbs of rats crossing a horizontal ladder with irregularly spaced rungs was assessed (Metz and Whishaw, 2002; Zorner *et al*., 2010). The percentage of functional placements, i.e. weight-bearing steps without slipping, was used as a parameter and reported for each limb separately. For swimming, the mean swimming velocity was calculated from at least three swims (swimming distance of 60 cm per run) per time point. The MTP peak velocity was defined as the maximal velocity of toe movement during hindlimb strokes.

After Week 12 post-lesion, rats with spinal cord injury ($n = 15$) used for the characterization of recovery after hemisection injury (Fig. 1) were further trained on the locomotor tasks (over-ground walking, wading and swimming) once a week. These rats received an electrolytic microlesion to either the ipsilesional ($n = 5$) or the contralesional ($n = 10$; one rat had to be excluded retrospectively due to incorrect positioning of the lesion) gigantocellular reticular nucleus (with reference to the side of the hemisection) 16 weeks after spinal cord injury. Rats without hemisection ($n = 7$) but electrolytic microlesion of the left gigantocellular reticular nucleus served as controls. Functional performance was assessed 1 day before and 2 days after the focal brainstem lesion.

Retrograde tracing from the spinal cord

Intact and spinal cord injured rats were deeply anaesthetized (Hypnorm/Dormicum, see above) and fixed in a stereotactic frame after partial laminectomy of the C5, C6 and C7 (spinal segments C6–T1) and T12 and T13 vertebrae (spinal segments L1–L4) (Gelderd and Chopin, 1977). Rats with hemisection injury received unilateral injections of two different fluorescent retrograde tracers into the ipsilesional cervical (tetramethylrhodamine, 3000 MW dextran; 10% in injectable water; Invitrogen) and ipsilesional lumbar spinal cord (diamidino yellow dihydrochloride, 2% suspension in 0.1 M phosphate buffer and 2% dimethylsulphoxide; Sigma-Aldrich) at 1 week ($n = 5$), 4 weeks ($n = 10$) or 12 weeks post-lesion ($n = 10$). Intact rats ($n = 5$) were traced accordingly. Injections were made stereotactically with Nanofil syringes attached to a MicroPump (WPI). A total of 2 µl of tetramethylrhodamine administered through 10 stereotactic injections of 200 nl was injected with a 33-gauge needle along the cervical spinal cord (700 µm lateral from the spinal cord midline, in a depth of 1 mm from the dorsal surface and a spacing of 1 mm between injections). Similarly, a total of 2 µl of diamidino yellow dihydrochloride was injected with a 28-gauge needle into the lumbar spinal hemicord (10 injections with 200 nl/injection, 500 µm lateral from the spinal cord midline, in a depth of 700 µm from the dorsal surface and a spacing of 1 mm between injections). Rats were perfused 14 days after tracing. Exclusive unilateral spread of the tracers was confirmed post-mortem for all injection sites on 40-µm thick spinal cord cross-sections under a fluorescence microscope. Coronal 40-µm thick cryostat sections of the whole brain and cross-sections of the spinal cord rostral to the lesion site were obtained for each rat. Prominent landmarks along the brains' rostrocaudal axis were used as a reference: the anterior commissure, the rostral end of the red nucleus, the central branch of the facial nerve, the rostral end of the inferior olive and the pyramidal decussation. Each brain region was identified using these landmarks and a rat brain atlas (Paxinos and Watson, 1998). Retrogradely labelled cell bodies were counted bilaterally in 19 different brain regions by a blinded experimenter. The same number of sections was analysed for each region and each rat. Single and

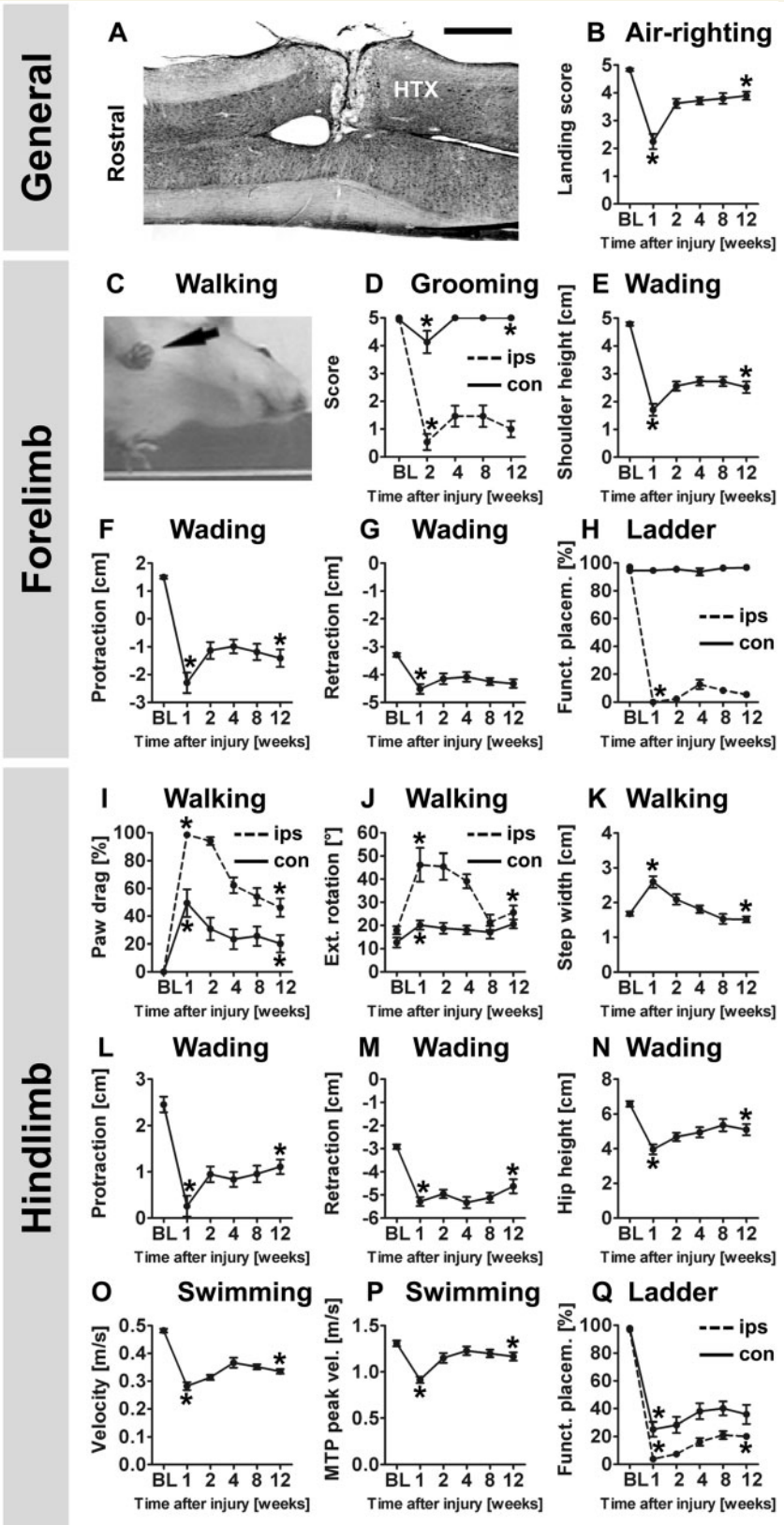

Figure 1 Functional outcome after cervical unilateral spinal cord injury. Motor performance of 15 rats was evaluated before (baseline, BL) and at several time points (1, 2, 4, 8 and 12 weeks) after unilateral hemisection injury at cervical level C4. (**A**) Nissl staining of a horizontal longitudinal spinal cord section illustrating the lesion paradigm used. Scale bar = 1 mm. (**B**) The air-righting reaction before and after injury was assessed with the landing score ranging from 0 (no reaction) to 5 (full rotation). (**C–H**) Performance of the forelimbs was evaluated during walking, grooming, wading and walking over a horizontal ladder. (**C**) An image (bottom view) of an injured rat during over-ground

(continued)

double labelled cell bodies were quantified on every fourth brain section (i.e. one section per 160 μm) under a fluorescence microscope and the result was multiplied by four to approximate the actual number of traced neurons. In the present study, we report absolute cell numbers for each region (Supplementary Tables 1–3). However, since absolute cell counts demonstrated high within-group variability due to the tracing procedure, absolute cell numbers for a given region were normalized to the total number of retrogradely labelled cells of the respective brain for each tracer.

Rostrocaudal coordinates ('+' rostral to landmark, '−' caudal to landmark) used for the individual regions were: the rostral motor cortex (start at 4800 μm + anterior commissure, end at 2560 μm + anterior commissure, total 2240 μm), the caudal motor cortex (start at 2560 μm + anterior commissure, end at 4640 μm − anterior commissure, total 7200 μm), the secondary somatosensory cortex (start at 1120 μm + anterior commissure, end at 4640 μm − anterior commissure, total 5760 μm), the red nucleus (start at red nucleus, end at 1920 μm − red nucleus, total 1920 μm), the deep mesencephalic reticular formation (start at 1280 μm + red nucleus, end at 1920 μm − red nucleus, total 3200 μm), the pontine reticular nucleus, oral part (start at 1920 μm − red nucleus, end at 1120 μm + facial nerve, total 2080 μm), the pontine reticular nucleus, caudal and ventral part (start at 1120 μm + facial nerve, end at facial nerve, total 1120 μm), the gigantocellular reticular nucleus (start at 160 μm − facial nerve, end at 1440 μm − inferior olive, total 3200 μm), the lateral paragigantocellular nucleus, the gigantocellular reticular nucleus (ventral part) and the gigantocellular reticular nucleus part alpha (start at 160 μm − facial nerve, end at 1440 − inferior olive, total 3200 μm), the dorsal paragigantocellular nucleus (start at 320 μm − facial nerve, end at 320 μm + inferior olive, total 1440 μm), the medullary reticular nucleus, ventral part (start at 1440 μm − inferior olive, end at pyramidal decussation, total 1440 μm), the medullary reticular nucleus, dorsal part (start at 800 μm − inferior olive, end at pyramidal decussation, total 1920 μm), the medial vestibular nucleus (start at 320 μm + facial nerve, end at 1440 μm − inferior olive, total 3680 μm), the lateral vestibular nucleus (start at 160 μm − facial nerve, end at 320 μm + inferior olive, total 1600 μm), the locus coeruleus (start at 1760 μm + facial nerve, end at facial nerve, total 1920 μm), the raphe magnus nucleus (start at 480 μm + facial nerve, end at inferior olive (IN), total 2560 μm), the raphe obscurus nucleus (start at 640 μm + inferior olive, end at pyramidal decussation, total 3520 μm) and the raphe pallidus nucleus (start at 160 μm + inferior olive, end at 640 μm + pyramidal decussation, total 2080 μm).

For propriospinal neurons located in the rostral cervical spinal cord at C3 and C4 level, labelled neurons were counted on every second to third spinal cord cross-section (thickness of 40 μm). As the number of analysed sections was different for each spinal segment and rat (10–40 sections per segment), the mean number of labelled cells per section was calculated. One intact rat was traced bilaterally from the cervical and lumbar spinal cord and each brain region analysed in the present study was reconstructed in 3D using Neurolucida 8.0 (MicroBrightField).

Anterograde tracing of reticulospinal fibres

Rats with cervical unilateral hemisection injury ($n = 15$) received a single stereotactic injection of 50 nl of the tracer mini-emerald (Fluorescin and biotin tagged 10 000 MW dextran, 10% in injectable water; Invitrogen) into the contralesional gigantocellular reticular nucleus 4 weeks after injury. Using a dorsal approach via the cerebellum, a 35-gauge needle was placed slightly dorsolaterally to the centre of the gigantocellular reticular nucleus (4.6 mm caudal to lambda, 1.5 mm lateral to lambda, 2 mm above the base of the skull) to avoid diffusion of the tracer over the midline and damage to the target neurons. In intact rats ($n = 10$, two rats were excluded due to incorrect tracing), the left gigantocellular reticular nucleus was traced accordingly. All rats were sacrificed 3 weeks after tracing and accurate placement of the injections was confirmed post-mortem. Series of 40-μm thick cryostat cross-sections of the cervical (C6–T1) and lumbar (L1–L6) spinal cord were analysed under a fluorescence microscope (every fourth section, 10 sections per segment). We counted fibres entering the contralesional (left for intact rats) spinal cord grey matter, midline crossing fibres and fibres in the ipsilesional (right for intact rats) grey matter. The latter were defined as fibres intersecting a virtual vertical line

Figure 1 Continued
walking 4 weeks after lesion shows that the digits of the ipsilesional forepaw (arrows) are contracted and form a clenched fist while the digits of the contralesional paw are spread and achieve full ground contact. (**D**) Grooming function was assessed for the ipsilesional (ips) and contralesional (con) forelimb separately using a scoring system ranging from 0 (no contact between paw and face) to 5 (grooming of the whole head and neck). (**E**) Shoulder height during wading was determined at midstance of the forelimb gait cycle. (**F** and **G**) Horizontal excursions of the ipsilesional forelimb were described via the maximal protraction (maximal *x*-value) and retraction (minimal *x*-value) of the wrist relative to the shoulder. (**H**) Precise targeting and placement of the ipsi- and contralesional forepaw was evaluated on a horizontal ladder. The percentage of functional placements (Funct. placem.), i.e. weight bearing steps without slipping, was used as a parameter to assess skilled locomotion. (**I–Q**) Performance of the hindlimbs was evaluated during walking, wading, swimming and walking over a horizontal ladder. (**I**) During over-ground walking the number of toe drags were counted for the ipsi- and contralesional hindlimb and counts were expressed as a percentage of steps with paw dragging. Also, external (Ext) rotation of the ipsi- and contralesional paw (**J**) and base of support (step width; **K**) was quantified during walking. Base of support was calculated by adding the distances measured between both heels and the body axis during stance phase for consecutive left-right hindlimb steps. (**L** and **M**) Horizontal excursions of the ipsilesional hindlimb during wading were described via the maximal protraction (maximal *x*-value) and retraction (minimal *x*-value) of the toe relative to the hip. (**N**) The hip height during wading was measured at midstance of the hindlimb gait cycle. Overall swimming speed (**O**) and the peak velocity of the ipsilesional metatarsophalangeal joint (MTP; **P**) were assessed during swimming. (**Q**) On the horizontal ladder, precise placement of the ipsi- and contralesional hindpaw was quantified as described for the forelimbs. Line graphs show group mean values for each time point ± SEM. For differences between time points, repeated measures one-way ANOVA followed by Bonferroni's Multiple Comparison Test was performed. Based on *post hoc* analysis, $*P < 0.05$ indicates significantly different values between baseline and Week 1 (or Week 2 for grooming) after injury (lesion effect) and between Week 1 (or Week 2 for grooming) and Week 12 post-lesion (recovery).

placed in the centre of the spinal cord grey matter at a distance of 600 μm from the central canal. To account for the variability induced by the tracing procedure, normalization was performed (Starkey *et al*., 2012; Lindau *et al*., 2014). Therefore, the number of midline-crossing fibres was normalized to the number of fibres entering the contralesional/left spinal cord grey matter for each segment. To assess the degree of arborization of reticulospinal fibres crossing the midline, the number of fibres counted in the ipsilesional/right spinal cord grey matter (see above) was divided by the number of midline-crossing fibres.

Retrograde tracing from the gigantocellular reticular nucleus

As described for anterograde tracing, intact rats ($n = 10$) and rats with chronic hemisection injury ($n = 10$, 4 weeks after injury) received stereotactic tracer injections into the ipsilesional (right in intact rats) and contralesional (left in intact rats) gigantocellular reticular nucleus. Tetramethylrhodamine (3000 MW dextran; Invitrogen) was injected into the ipsilesional/right and mini-emerald (10 000 MW dextran; Invitrogen) into the contralesional/left nucleus. Correct positioning of the needle was checked for each injection site and injections that were off target were excluded from further analysis. For the rostral cortex, retrogradely-labelled cells were counted on every second 40-μm thick coronal section (in total 17 sections per rat, starting at the most rostral section with labelled cells). For the MLR, labelled cells were quantified in the area (1.4 mm^2) of the cuneiform and pedunculopontine nucleus located laterally to the mesencephalic trigeminal neurons. Again, cells were counted in this area on every second 40-μm thick coronal section (in total 12 sections per rat). To normalize for differences in tracing efficiency cell counts were expressed as a lateralization index (number of cells contralateral to injection/number of cells ipsilateral to injection).

Focal lesions of the gigantocellular reticular nucleus

Rats received a local, anodal, electrolytic lesion of the gigantocellular reticular nucleus in the rostral medulla oblongata using platinum-iridium electrodes (118 kΩ; Science Products,) attached to a stereotactic frame. The tip of the electrode was placed in the ventromedial part of the gigantocellular reticular nucleus, 4.6 mm caudal to lambda, 1 mm lateral to lambda and 1.5 mm above the base of the skull. An electric current of 200 μA was applied continuously for 35 s. Only data obtained from rats with histologically confirmed accurate positioning of the lesion were analysed.

Statistics

Statistical analysis was performed using SPSS (V21; SPSS, Inc) and GraphPad Prism 5 (V5.01; GraphPad Software, Inc). The level of statistical significance for all tests was set *a priori* at $P < 0.05$. The exact *P*-values obtained from statistical analyses are given. For analysis of the behavioural data characterizing the time course after spinal cord injury (Fig. 1), we used one-way ANOVA for repeated measurements. If significant, ANOVA was followed by *post hoc* Bonferroni's Multiple Comparison Test comparing the performance at baseline and 1 week (or 2 weeks for grooming) after injury ('lesion effect') and 1 week (or 2 weeks for grooming) and 12 weeks after injury ('recovery'). For retrograde tracing from the cervical and lumbar spinal cord (Figs 3 and 4), the absolute numbers of retrogradely labelled neurons found in a given CNS region were normalized to the total cell number counted per brain (for the same tracer) to reduce within-group variability due to tracing. Statistical analysis on the number of normalized cell counts was performed with one-way ANOVA and followed, if significant, by Bonferroni's Multiple Comparison Test. For anterograde tracing from the contralesional gigantocellular reticular nucleus (Fig. 5), repeated measures two-way ANOVA with one repeated factor ('Segment') and one non-repeated factor ('Injury') was applied to detect significant differences between each spinal cord segment and between intact rats and rats with hemisection injury. Total mean values were analysed with Student's unpaired *t*-test (two-sided). For changes of the lateralization index (Fig. 6), one-way ANOVA was used to test for significant differences between animal groups. Here, repeated measures ANOVA could not be applied because of the differences in group size due to the exclusion of inaccurate injection sites. If significant, ANOVA was, again, followed by Bonferroni's Multiple Comparison Test. For statistical analysis of the behavioural effects of microlesions in the brainstem (Fig. 7), repeated measures two-way ANOVA with one repeated factor ('Time', i.e. before and after brainstem lesion) and one non-repeated factor ('animal group') was used. Only if ANOVA was significant for the repeated measures factor 'Time', *post hoc* analysis was performed with Bonferroni's Multiple Comparison Test (Supplementary Table 4).

Results

Behavioural outcome after cervical unilateral spinal cord injury

Adult Lewis rats were tested for their paw preference in the cylinder test and results indicated equal use of both paws (data not shown). After several days of training and baseline testing in a number of behavioural tasks (see below), all rats received a hemisection injury at cervical level C4 (Fig. 1A). Only data from rats with a histologically confirmed complete hemisection ($n = 15$) were included in the analysis.

The air-righting reaction (Fig. 1B), i.e. the ability to turn in the air from a supine position in order to land on the paws, was strongly impaired 1 week after injury ($P < 0.0001$, repeated measures one-way ANOVA). At this time point, rats were only just able to rotate their head and shoulder girdle and occasionally their hindlimbs before landing. This was followed by significant recovery of this response starting 1–2 weeks after lesion ($P < 0.0001$, repeated measures one-way ANOVA).

Forelimbs

The ipsilesional, right forepaw was rigid and with flexed, contracted digits (Fig. 1C). Starting 2–4 weeks after lesion, rats used their ipsilesional forelimb like a 'walking stick' with only minimal movements in the elbow and wrist, as described previously (Zorner *et al*., 2010; Filli *et al*., 2011). All assessed parameters including grooming scores (Fig. 1D), shoulder height (Fig. 1E) and limb excursions (Fig. 1F and G) as well as precise paw placement on the horizontal ladder (Fig. 1H) indicated very severe deficits in the ipsilesional forelimb acutely after lesion. Starting 2 weeks post-lesion, a small but significant degree of improvement of crude forelimb movements, such as increased shoulder height

(Fig. 1E) and limb protraction (Fig. 1F), occurred ($P < 0.0001$, repeated measures one-way ANOVA). However, performance of the ipsilesional forelimb in general, and on the horizontal ladder in particular, remained far below baseline levels up to 12 weeks post-lesion (<20% of baseline performance) indicating persistent deficits of distal forelimb function. The contralesional forelimb was not significantly affected by the lesion (Fig. 1H; $P = 0.45$, repeated measures one-way ANOVA).

Hindlimbs

Hindlimbs demonstrated moderate to severe deficits acutely after cervical hemisection injury with the ipsilesional hindlimb being more affected than the contralesional one in most of the behavioural tasks. Locomotor parameters assessed during over-ground walking [toe clearance (Fig. 1I), paw rotation (Fig. 1J), base of support (Fig. 1K)], wading through shallow water [hindlimb excursion (Fig. 1L and M), hip height (Fig. 1N)] and swimming [swimming velocity (Fig. 1O), maximal toe velocity during hindlimb strokes (Fig. 1P)] showed significant recovery, often close to pre-lesion levels, 4–12 weeks after spinal cord injury [for all parameters $P < 0.01$, repeated measures one-way ANOVA, except for paw rotation of the contralesional hindlimb (Fig. 1J)]. Precise paw placement on the horizontal ladder was initially very poor for both hindlimbs illustrated by 20–40% (contralesional limb) and <10% (ipsilesional limb) functional paw placements on the ladder rungs 1 week after lesion (Fig. 1Q). In contrast with the good recovery of basic locomotor functions, only limited recovery was observed for both hindlimbs on the horizontal ladder.

Anatomical plasticity of spinal descending tracts after spinal cord hemisection assessed by retrograde tracing

Cervical (C4) hemisection disrupts all descending tracts on the lesioned side. To re-establish functional control over the denervated spinal hemicord below the lesion, fibres from the intact side may sprout across the spinal cord midline or activate pre-existing midline crossing axonal branches. This was studied by injecting retrograde neuroanatomical tracers with different colours into the denervated ipsilesional cervical and lumbar spinal cord grey matter below the lesion (Fig. 2A). These tracers were taken up very efficiently by axon terminals, transported retrogradely and accumulated in the cell bodies. Four groups of rats received such tracer injections: (i) intact rats ($n = 5$); (ii) rats traced 1 week after injury ($n = 5$); (iii) rats traced 4 weeks after injury ($n = 10$) and; (iv) rats traced 12 weeks after injury ($n = 10$). Retrogradely labelled cell bodies were counted bilaterally in 19 different brain regions (Fig. 2B–E) and in the cervical spinal cord rostral to the injury. Although stereotactic tracer injections were performed identically for all rats, absolute cell counts showed high within-group variability (Supplementary Tables 1–3). Therefore, cell counts for a given region were normalized to the total number of retrogradely labelled cells of the respective brain (Figs 3 and 4).

After retrograde tracing from the denervated ipsilesional cervical spinal cord below the lesion (Fig. 3), we found a significant increase of labelled normalized cells in the contralesional gigantocellular reticular nucleus at 4 weeks after injury compared to the acute state ($P = 0.023$, one-way ANOVA). In terms of absolute numbers, we found 345 ± 146 labelled cells in the contralesional gigantocellular reticular nucleus in rats traced 1 week after injury compared to 402 ± 158 and 685 ± 280 labelled cells in those rats traced 4 and 12 weeks post-lesion, respectively (Supplementary Table 1). There was a tendency for higher cell numbers in the ipsilesional red nucleus (17 ± 11 cells at 1 week versus 59 ± 20 cells at 12 weeks after lesion, Supplementary Table 1) and the contralesional locus coeruleus (50 ± 50 cells at 1 week versus 104 ± 61 cells at 12 weeks after lesion, Supplementary Table 1), however, with large interindividual variations. Spinal projections to the denervated cord were unchanged for the cortex, other reticular nuclei and the vestibular nuclei. The number of raphe neurons projecting to the denervated cervical hemicord from the contralesional raphe was reduced 4 weeks after injury ($P = 0.026$, one-way ANOVA; Fig. 3). After retrograde tracing from the lumbar denervated hemicord (Fig. 4), we again found significantly higher normalized cell numbers in the contralesional gigantocellular reticular nucleus in the chronic rats ($P = 0.041$, one-way ANOVA). Accordingly, absolute cell numbers for the contralesional gigantocellular reticular nucleus increased from 434 ± 119 labelled cells at 1 week after injury to almost twice the amount at 4 and 12 weeks post-lesion (Supplementary Table 2). Also, normalized cell numbers were increased in the ipsilesional dorsal medullary reticular nucleus 12 weeks after injury compared to rats traced 1 week after hemisection ($P = 0.0016$, one-way ANOVA; Fig. 4). Again, the number of normalized cells in the raphe nuclei was reduced in chronic rats after lumbar tracing, however, this time, statistical significance was found for the ipsilesional side ($P < 0.0226$, one-way ANOVA; Fig. 4). There was a tendency for increased projections to the denervated lumbar hemicord from the contralesional cortex and pontine reticular nuclei. No significant changes were detected for the other brain regions. Most double-labelled cells, i.e. cells with collaterals in the cervical and lumbar spinal cord, were found in the pontine and medullar reticular formation in intact rats (Supplementary Table 3). After hemisection, the number of double-labelled cells counted in the contralesional reticular formation increased proportionally with the number of single-labelled neurons. Absolute cell counts for all analysed brain and spinal cord regions are given in Supplementary Tables 1–3.

In summary, these retrograde tracing results show plastic reactions in some but not all brainstem regions. In particular, this is seen in the contralesional gigantocellular reticular nucleus with many neurons whose axons cross the spinal cord midline in response to the hemisection injury. Anterograde tracing of this nucleus was performed to directly visualize these axons.

Anterograde tracing of reticulospinal projections of the gigantocellular reticular nucleus

Intact rats ($n = 8$) and rats with chronic cervical unilateral hemisection injury ($n = 15$; 4 weeks after lesion) received a stereotactic tracer injection into the contralesional (left nucleus in intact rats) gigantocellular reticular nucleus [Fig. 5A(I–III)]. Traced fibres

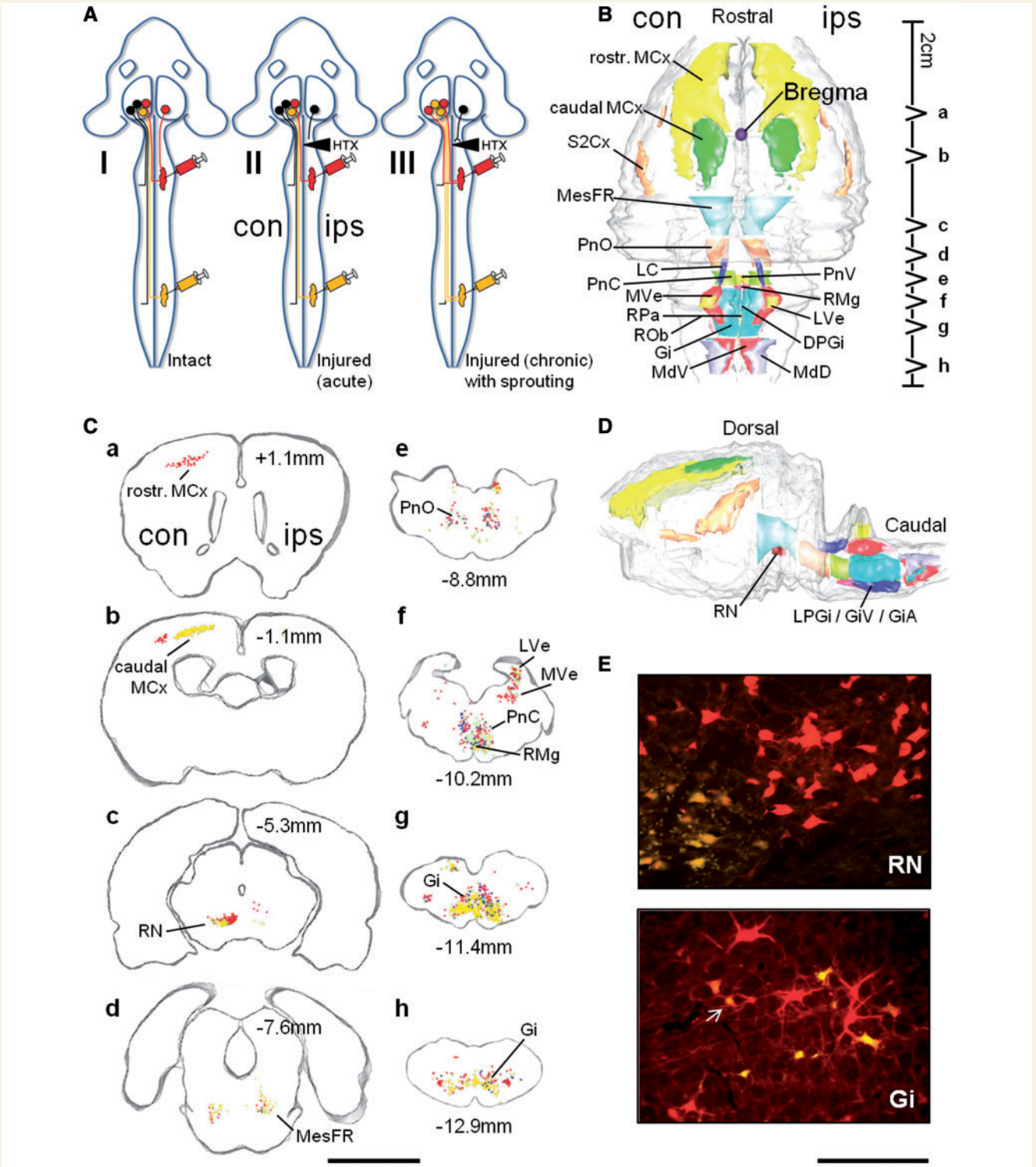

Figure 2 Retrograde tracing of brain regions with spinal projections. (**A**) Scheme illustrating the experimental approach. (**A**, **I**) Rats received unilateral spinal injections of two different fluorescent retrograde tracers. Tetramethylrhodamine (red) and diamidino yellow dihydrochloride (yellow) were injected into the cervical (C5–T1) and lumbar spinal cord grey matter (L1–L6), respectively. Tracers were taken up by axon terminals and transported retrogradely, eventually accumulating in the corresponding cell bodies. Under a fluorescent microscope, neurons projecting into the injected cervical spinal hemicord appeared red while cells with projections into the injected lumbar hemicord were yellow. For the cervical spinal cord, a crossed and uncrossed pathway is illustrated. Neurons without terminals contacting the injection sites remained non-fluorescent (black cells). (**A**, **II**) After unilateral hemisection injury at C4 (HTX), cells located in the ipsilesional half of the CNS with exclusively ipsilateral descending projections lost access to the injection sites due to axotomy and were not labelled (right black cell). (**A**, **III**) A neuron that changed its spinal projection pattern in response to injury, i.e. sprouting over the midline at cervical or lumbar spinal segments below the lesion site, gained access to the tracer and might be labelled accordingly (one black cell on

(continued)

entering the contralesional spinal cord grey matter, midline-crossing fibres and fibres in the ipsilesional, denervated grey matter at lower cervical (C6–T1) and lumbar (L1–L6) spinal levels were assessed [Fig. 5B(I–IV)]. In general, there were significantly more midline-crossing fibres in the lumbar spinal cord than in the cervical segments ($P = 0.0003$ for the factor 'Segment', repeated measures two-way ANOVA; Fig. 5C). Compared with intact rats, we found a significant increase of the number of midline-crossing fibres for all segments in rats with spinal cord injury ($P = 0.0444$ for the factor 'Injury', repeated measures two-way ANOVA; Fig. 5C). In intact rats, there were 1–2 fibres in the ipsilesional spinal cord grey matter [Fig. 5B(IV)] per midline crossing fibre. These fibres were primarily found in the ventral spinal cord grey matter in intact and lesioned animals. After spinal cord injury, there was a tendency towards a reduction of fibres in the ipsilesional cervical spinal cord per midline-crossing fibre but an unchanged ratio in the lumbar spinal cord (Fig. 5D).

These findings from anterograde tracing confirmed the previous results of the retrograde tracing experiments demonstrating sprouting of spinal projections of the contralesional gigantocellular reticular nucleus across the spinal cord midline to the denervated side after hemisection. We therefore investigated whether plastic changes including a side-switch were also present in the input systems to the contralesional gigantocellular reticular nucleus in response to spinal cord injury.

Retrograde tracing of the inputs of the gigantocellular reticular nucleus

Intact rats ($n = 10$) and rats 4 weeks after cervical unilateral hemisection ($n = 10$) received stereotactic injections of the fluorescent tracers mini-emerald (green) into the contralesional (left in intact rats) and tetramethylrhodamine (red) into the ipsilesional (right in intact rats) gigantocellular reticular nucleus. In intact rats, retrogradely labelled cell bodies were found primarily in the reticular formation in the midbrain, pons and medulla oblongata on both sides, as well as in the forebrain cortex. Two brain regions that are functionally and anatomically closely linked to the gigantocellular reticular nucleus were analysed in detail: the rostral motor cortex (Antal, 1984; Matsuyama *et al*., 2004), containing the rostral forelimb area and also considered as the premotor region in rats (Passingham *et al*., 1988; Rouiller *et al*., 1993; Smith *et al*., 2010) and the MLR, a phylogenetically ancient and highly conserved command centre for locomotion (Steeves and Jordan, 1984; Garcia-Rill *et al*., 1986) [Fig. 6A(I–IV)]. Based on retrogradely labelled cell counts in intact rats, we found that the gigantocellular reticular nucleus received bilateral projections from the rostral motor cortex with about two-thirds of the traced neurons located in the contralateral and one-third in the ipsilateral cortex [Fig. 6A(I and III)]. Projections from the MLR were also bilateral, but with stronger ipsilateral than contralateral projections [Fig. 6A(II and IV)]. As analysis of absolute cell numbers revealed high within-group variability for the same retrograde tracer, and tracers showed different tracing efficiencies, we calculated a lateralization index for each traced region as a measure for contra- versus ipsilateral innervation [Fig. 6B(I and II)]. Compared with intact rats, no statistically significant changes of the projection pattern between the rostral motor cortex and the ipsi- and contralesional gigantocellular reticular nucleus were found as a consequence of spinal cord injury [Fig. 6B(I)]. However, for the MLR, the lateralization index for projections to the contralesional gigantocellular reticular nucleus increased significantly after hemisection injury [$P = 0.0302$, one-way ANOVA; Fig. 6B(II)]. These results suggest that spinal sprouting of reticulospinal fibres originating from the contralesional gigantocellular reticular nucleus is accompanied by modifications of its supraspinal input after spinal hemisection.

Behavioural changes after micro-lesioning of the gigantocellular reticular nucleus in rats with chronic spinal cord injury

To assess the functional relevance of the observed anatomical changes in the reticular mesencephalic-medullar-spinal system, rats

Figure 2 Continued
the left turned red and the other one yellow in the scheme). con = contralesional (left-side in intact rats); ips = ipsilesional (right-side in intact rats). (**B**) Three-dimensional Neurolucida reconstruction of a rat brain (no lesion) based on bilateral retrograde tracings from the cervical and lumbar spinal cord illustrating the regions analysed, dorsal view. Rostr. MCx = rostral motor cortex; caudal MCx = caudal motor cortex; S2Cx = secondary somatosensory cortex; MesFR = deep mesencephalic reticular formation; PnO = pontine reticular nucleus, oral part; LC = Locus coeruleus; PnC = pontine reticular nucleus, caudal part; MVe = medial vestibular nucleus; RPa = raphe pallidus nucleus; ROb = raphe obscurus nucleus; Gi = gigantocellular reticular nucleus; MdV = medullary reticular nucleus, ventral part; MdD = medullary reticular nucleus, dorsal part; DPGi = dorsal paragigantocellular nucleus; LVe = lateral vestibular nucleus; RMg = raphe magnus nucleus; PnV = pontine reticular nucleus, ventral part. (**C**) Coronal brain slices of an intact rat reconstructed with Neurolucida after right-sided ('ips') unilateral tracing from the cervical and lumbar spinal cord, as illustrated in **A**. Each coronal plate shown (**a**–**h**) resulted from the reconstruction of four consecutive brain slices with a thickness of 40 µm. The location of each coronal plate is indicated by the anterioposterior distance to bregma and also illustrated in **B**. Red cell bodies were traced with tetramethylrhodamine (cervical injections), yellow cell bodies were labelled with diamidino yellow dihydrochloride (lumbar injections) and purple cells were double-labelled. Scale bar = 5 mm. Abbreviations as in **B**. (**D**) Three-dimensional Neurolucida reconstruction of analysed brain regions, lateral view. RN = red nucleus; LPGi = lateral paragigantocellular nucleus; GiV = gigantocellular reticular nucleus, ventral part; GiA = gigantocellular reticular nucleus, alpha part. (**E**) Fluorescence microscopy images of selected brain regions after unilateral cervical (tetramethylrhodamine, red cells) and lumbar (diamidino yellow dihydrochloride, yellow cells) tracing. Note the somatotopic organization of the red nucleus (RN) and the presence of double-labelled cells (arrow) in the gigantocellular reticular nucleus (Gi). Scale bar = 200 µm.

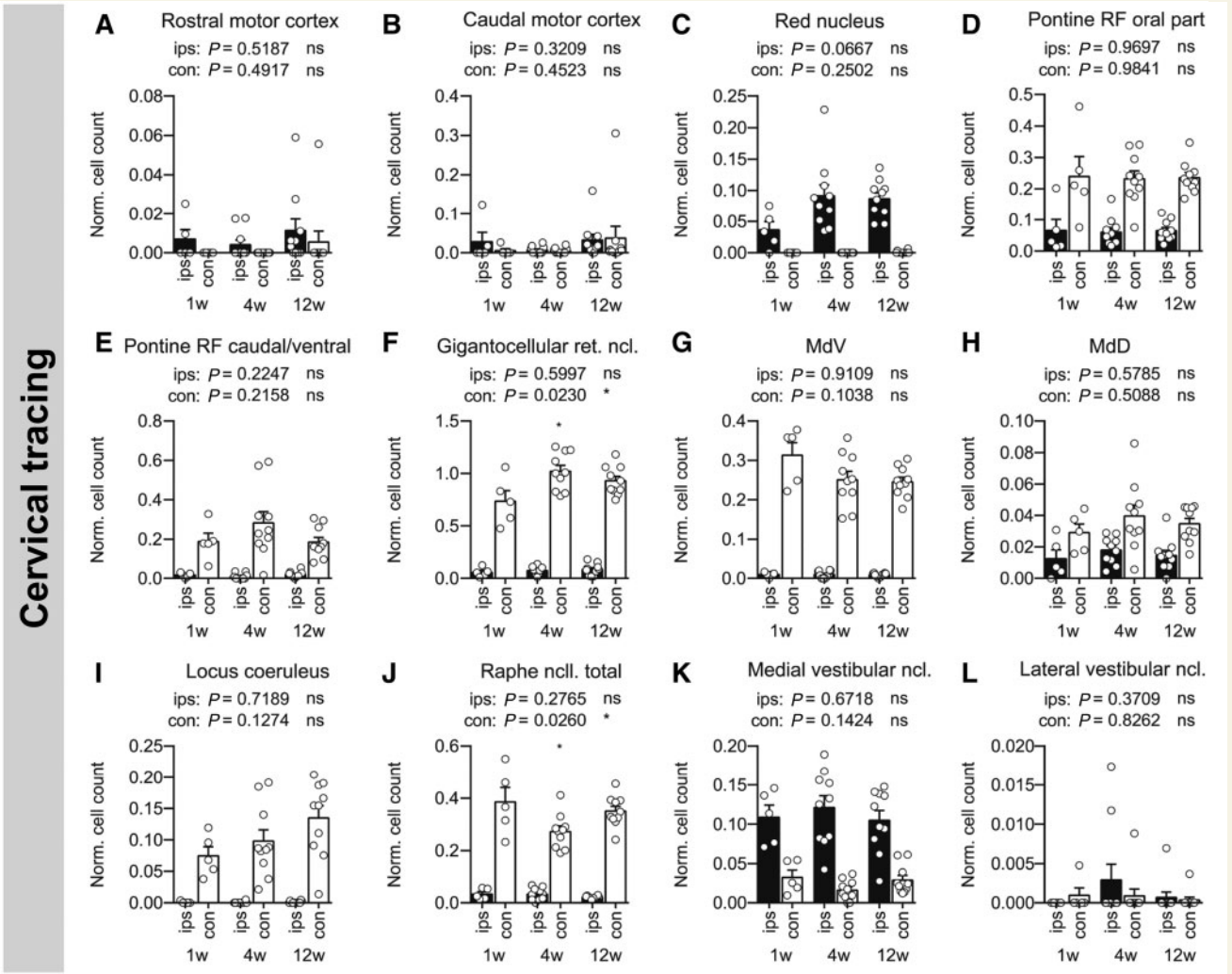

Figure 3 Normalized results of retrograde tracing from the ipsilesional cervical hemicord. Normalized cell counts for rats traced 1 ($n = 5$), 4 ($n = 10$) and 12 ($n = 10$) weeks after unilateral hemisection are presented for a number of selected brain regions. Retrograde tracing was performed from the cervical spinal cord as illustrated in Fig. 2A. Circles represent single animals. Bars show total group mean values for each time point ± SEM. For differences between time points, one-way ANOVA followed by Bonferroni's Multiple Comparison Test was performed. Exact *P*-values derived from the ANOVA are given above the graphs with $*P < 0.05$ indicating significantly different normalized cell counts between time points. Results from *post hoc* testing are illustrated in the graph with $*P < 0.05$ denoting significantly different values either between Week 1 and Week 4 (*above the 4 week column) or between Week 1 and Week 12 (not present in this figure) after injury. ns = not significant; con = contralesional; ips = ipsilesional; w = week; ret. = reticular; ncl. = nucleus; ncll. = nuclei; MdV = medullary reticular nucleus, ventral part; MdD = medullary reticular nucleus; RF = reticular formation.

were allowed to recover from unilateral cervical hemisection injury for a period of 16 weeks. Then, rats with spinal cord injury received electrolytic microlesions of either the ipsilesional ($n = 5$) or contralesional ($n = 9$) gigantocellular reticular nucleus (Fig. 7A and B). For comparison, intact rats of the same age ($n = 7$) were also trained on the behavioural tasks and received a microlesion of the left gigantocellular reticular nucleus. Functional testing was performed 1 day before and 2 days after the focal brainstem lesion. Following brainstem lesion, intact rats did not demonstrate any functional impairment (Fig. 7C–Q and Supplementary Table 4).

Rats with chronic hemisection injury and acute damage to the ipsilesional gigantocellular reticular nucleus showed a significantly reduced shoulder height during wading (see results of the repeated measures two-way ANOVA for all assessed parameters in Supplementary Table 4; Fig. 7C) and a significantly reduced toe clearance of both hindpaws during walking (Fig. 7F and G). There was a tendency towards an increased external rotation of the ipsilesional (referring to the side of the hemisection), but not the contralesional hindpaw (Fig. 7H and I). In these rats, a broader step width (Fig. 7J) was mainly due to a laterally displaced ipsilesional hindlimb (Fig. 7L).

Rats with chronic hemisection injury and acute damage to the contralesional gigantocellular reticular nucleus demonstrated similar functional deficits to those rats with acute damage to the

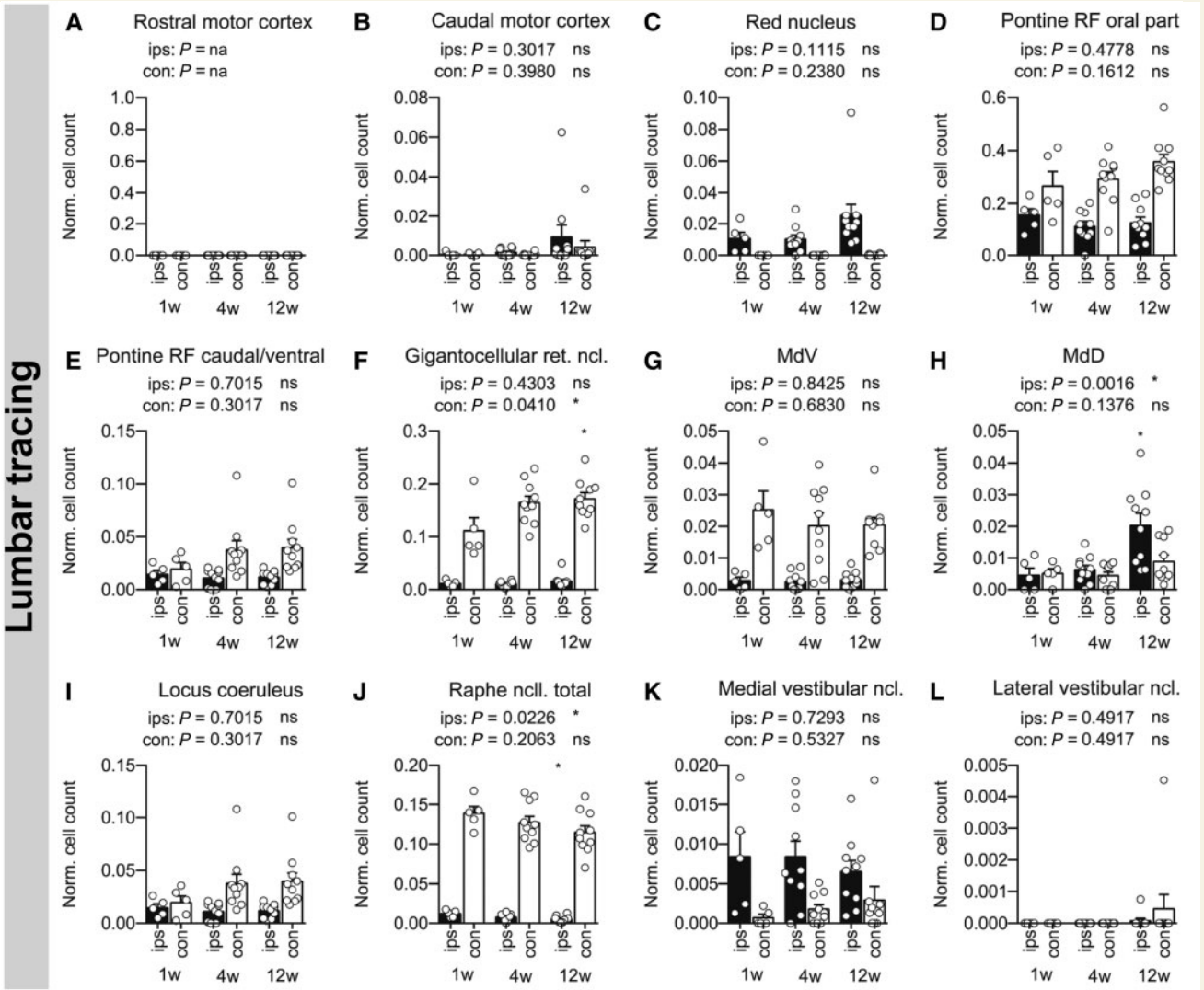

Figure 4 Normalized results of retrograde tracing from the ipsilesional lumbar hemicord. Normalized cell counts for rats traced 1 ($n = 5$), 4 ($n = 10$) and 12 ($n = 10$) weeks after unilateral hemisection are presented for the same brain regions as shown in Fig. 3. Retrograde tracing was performed from the lumbar spinal cord as demonstrated in Fig. 2A. Circles represent single animals. Bars show total group mean values for each time point ± SEM. For differences between time points, one-way ANOVA followed by Bonferroni's Multiple Comparison Test was performed. Exact *P*-values derived from the ANOVA are given above the graphs with $*P < 0.05$ indicating significantly different normalized cell counts between time points. Results from *post hoc* testing are illustrated in the graph with $*P < 0.05$ indicating significantly different values either between Week 1 and Week 4 (not present in this figure) or between Week 1 and Week 12 (*above the 12-week column) after injury. ns = not significant; na = not applicable; con = contralesional; ips = ipsilesional; w = week; ret. = reticular; ncl. = nucleus; ncll. = nuclei; MdV = medullary reticular nucleus, ventral part; MdD = medullary reticular nucleus; RF = reticular formation.

ipsilesional nucleus including reduced shoulder height during wading as well as dragging of both hindpaws, increased external rotation of the ipsilesional hindpaw and a broader step width during over-ground walking (Supplementary Table 4 and Fig. 7C–L). However, only rats with chronic spinal cord injury and damage to the contralesional gigantocellular reticular nucleus showed a significantly decreased swimming velocity and a reduced peak stroke velocity of the ipsilesional (again, referring to the side of the hemisection) hindlimb during swimming (Supplementary Table 4 and Fig. 7P and Q). Hip height and basic limb excursions (pro- and retraction) of the ipsilesional fore- and hindlimb during wading were not affected by focal brainstem lesions on either side (Fig. 7M–O). Thus, acute lesion of either the ipsi- or the contralesional gigantocellular reticular nucleus in rats with chronic hemisection injury affected bilateral hindlimb function. Damage to the contralesional gigantocellular reticular nucleus produced specific deficits of the ipsilesional hindlimb during swimming.

Discussion

In humans, unilateral spinal cord hemisection causes Brown-Séquard syndrome, which is known to be associated with good recovery of locomotor functions, but poor recovery of hand

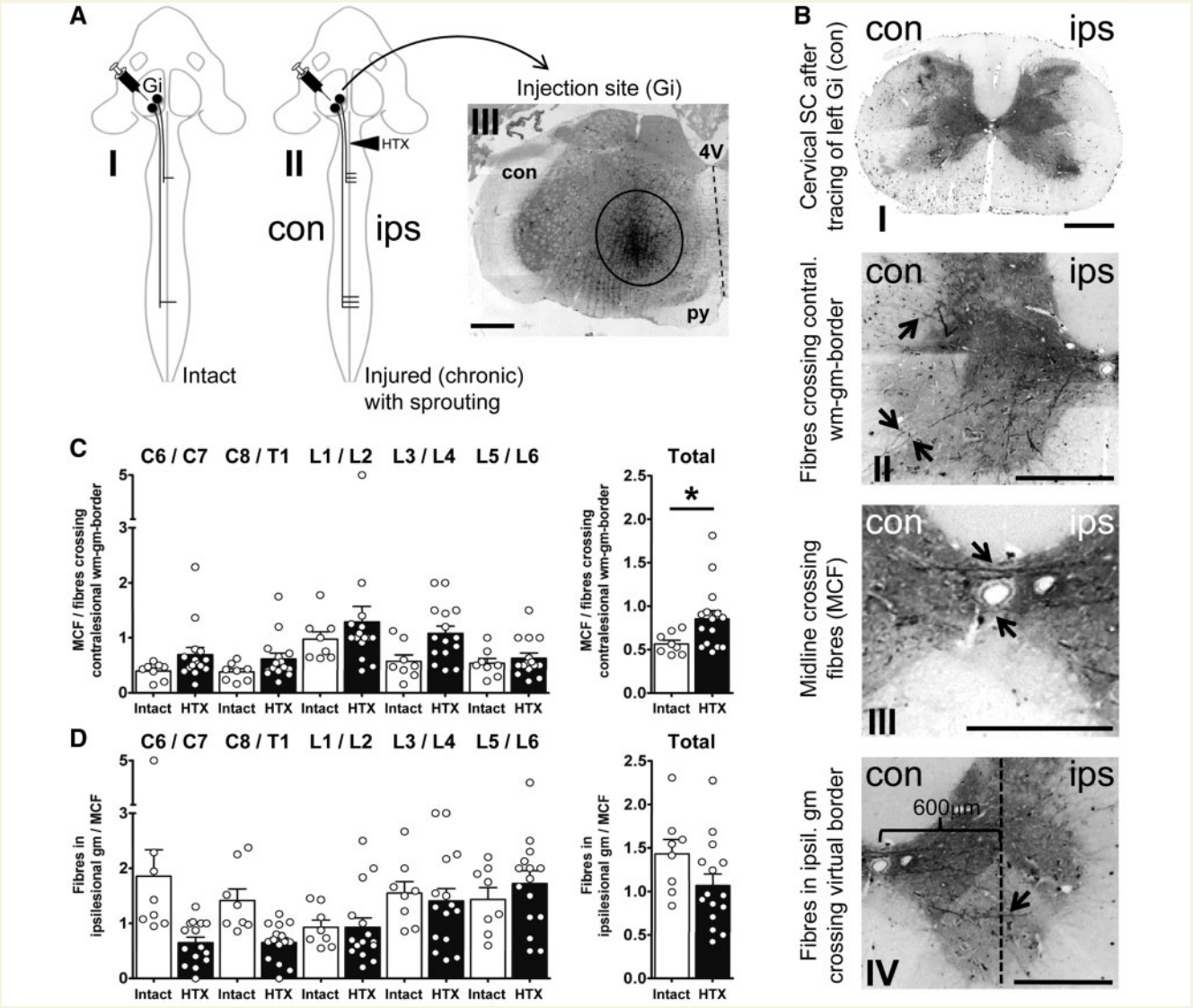

Figure 5 Anterograde tracing of reticulospinal projections from the contralesional gigantocellular reticular nucleus. (**A**) Scheme illustrating the anterograde tracing experiment. Intact rats (**A I**) and rats with chronic (4 weeks post-lesion; **A II**) cervical unilateral hemisection injury (HTX) received micro-injections of the anterograde tracer mini-emerald into the contralesional (left for intact rats) gigantocellular reticular nucleus (Gi). (**A III**) Fluorescence microscopy image of a brainstem cross section (thickness of 40 µm) demonstrating the injection site in an injured rat. The tracer was primarily visible in the region of the gigantocellular reticular nucleus (circle) and the needle tract. In all analysed rats, spreading of the tracer over the midline (dashed line) was not detected. Scale bar = 1 mm. Py = pyramidal tract; 4V = fourth ventricle. (**B I**) Fluorescence microscopy image of a cervical spinal cord cross-section of an intact rat after anterograde tracing of the left (con) gigantocellular reticular nucleus. Black dots in the spinal cord white matter are traced reticulospinal fibres. Note that we found mainly reticulospinal fibres descending in the ventral, ventrolateral and dorsolateral funiculus on the side of the tracer injection (con). Scale bar = 1 mm. (**B II–IV**) Fluorescence microscopy spinal cord images of high magnification of a lesioned rat showing traced fibres (arrows) entering the contralesional spinal cord grey matter (**B II**) as well as midline-crossing fibres (**B III**) and fibres passing a virtual border placed in the centre of the ipsilesional grey matter at a distance of 600 µm from the central canal (**B IV**). Scale bars = 500 µm. (**C** and **D**) Results of the anterograde tracing experiment in intact rats ($n = 8$) and rats with cervical unilateral hemisection injury ($n = 15$). The number of midline-crossing fibres normalized to the number of fibres entering the contralesional spinal cord grey matter (**C**) and the number of fibres in the ipsilesional grey matter per midline-crossing fibre (**D**) are presented as total mean value for all analysed segments and for the spinal cord segments C6-T1 and L1-L6 separately. Bars show group mean values ± SEM. Circles represent individual rats. For differences between groups, repeated measures two-way ANOVA was performed. Mean values (total) were analysed using unpaired two-tailed *t*-test with $*P < 0.05$ indicating significantly different results. con = contralesional (left side in intact rats); ips = ipsilesional (right side in intact rats). SC = spinal cord; Gi = gigantocellular reticular nucleus; wm = white matter; gm = grey matter.

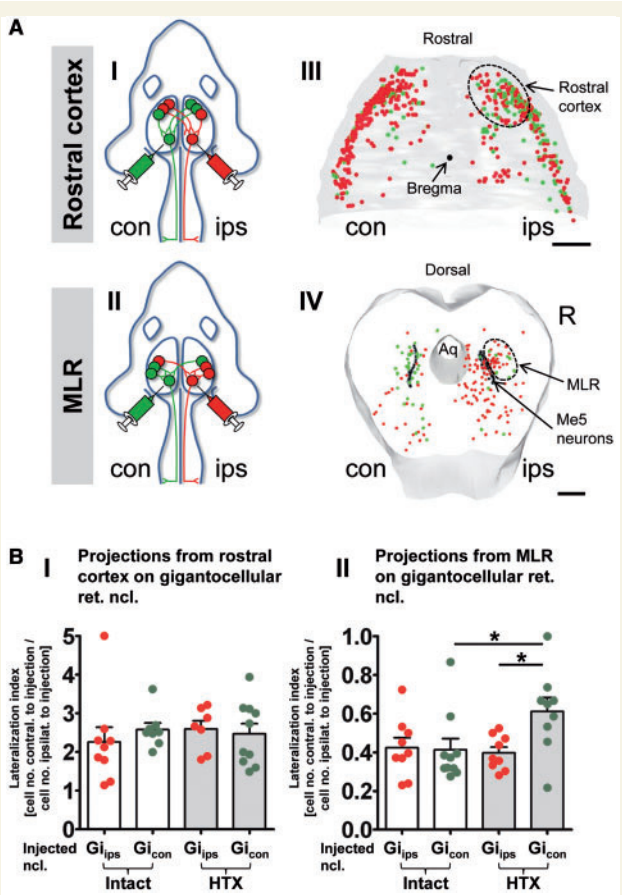

Figure 6 Retrograde tracing of the gigantocellular reticular nucleus. (**A I** and **II**) Scheme illustrating anatomical connections between the gigantocellular reticular nucleus and the rostral motor cortex (**A I**) and the MLR (**A II**) in an intact rat. (**A III** and **IV**) Three-dimensional Neurolucida reconstruction of the cortex and the midbrain of an intact rat after bilateral retrograde tracings from the left ('con', green cells) and right ('ips', red cells) gigantocellular reticular nucleus (**A III** dorsal view, scale bar = 2 mm; **A IV** frontal view, scale bar = 1 mm). Aq = aqueduct; Me5 = mesencephalic trigeminal nucleus (black dots); con = contralesional (left-side in intact rats); ips = ipsilesional (right-side in intact rats). (**B I** and **II**) Retrogradely labelled neurons in the rostral motor cortex (**B I**) and MLR (**B II**) were analysed using the lateralization index. Results are presented for intact rats ($n = 10$; intact; white bars) and rats with hemisection injury ($n = 10$; HTX; grey bars). Note that not all injections were placed correctly in the centre of the gigantocellular reticular nucleus. These injections were removed from analysis explaining differences in group size. Bars show group mean values ± SEM. For tracing from the ipsilesional (Gi_{ips}; right side in intact rats) and contralesional (Gi_{con}; left side in intact rats) gigantocellular reticular nucleus. Red and green dots represent single rats (colour code as in **A**). For differences between groups, one-way ANOVA followed by Bonferroni's Multiple Comparison Test was performed. $*P < 0.05$ indicates significantly different results. ret. = reticular; ncl. = nucleus.

movements (Little and Halar, 1985). The rat spinal cord injury model used in the present study reproduced these behavioural findings and showed anatomical plasticity in specific parts of the CNS following the cervical hemisection. The different descending motor tracts were found to vary greatly in their plastic responses; major changes were observed mainly in the medullary reticular system. Retrograde and anterograde tracing showed that reticulospinal fibres originating from the contralesional gigantocellular reticular nucleus sprouted across the spinal cord midline in response to the injury to innervate the denervated hemicord, in particular in the lumbar spinal cord (Fig. 8). These anatomical changes were accompanied by a high degree of recovery of basic locomotor functions which are believed to be at least partially mediated by the reticulospinal system innervating the spinal central pattern generators (Grillner, 1996; Matsuyama *et al*., 2004; Hagglund *et al*., 2010). Consistent with this, sparing of reticulospinal fibres after contusion injury was found to be associated with a better functional outcome (Basso *et al*., 2002). However, others failed to demonstrate an increase of reticulospinal midline-crossing fibres in rodents after spinal cord injury (Ballermann and Fouad, 2006; Courtine *et al*., 2008; Weishaupt *et al*., 2013). We believe that discrepancies between these and our experiments can be mainly attributed to methodological differences (tracing efficacy, type of lesion and analysis).

The rubrospinal system showed a tendency towards an increased number of fibres re-crossing the CNS midline which was, however, not statistically significant. Also, the corticospinal and vestibulospinal system demonstrated no statistically significant increase of midline-crossing fibres after hemisection. However, due to high within-group variability, the data do not allow us to draw the conclusion that these tracts did not respond to the lesion at all. In addition, we did not investigate other forms of anatomical plasticity, such as sprouting onto long propriospinal neurons or commissural interneurons that could also provide cortical reinnervation via detour circuits (Bareyre *et al*., 2004; Jankowska *et al*., 2006; Courtine *et al*., 2008). We observed a fast recovery of the air-righting reaction within a few days after injury. This reaction is triggered by signals from the labyrinth and mediated through the (lateral) vestibulospinal tract (Pellis *et al*., 1991). As recovery was not associated with significant sprouting of vestibulospinal axons over the midline below the lesion site, optimal use of the spared vestibulospinal-propriospinal connections may allow for rapid recovery of vestibulospinal function in a similar way as the crossed phrenic phenomenon (Goshgarian, 2003). The decrease of serotonergic projections to the denervated hemicord after hemisection is in-line with previous findings in the same spinal cord injury animal model (Filli *et al*., 2011) and may explain the beneficial effects of treatment with serotonergic agonists after spinal cord injury (Courtine *et al*., 2009).

After hemisection injury, the number of reticulospinal midline-crossing fibres increased in cervical as well as lumbar spinal segments suggesting growth promoting factors originating from the denervated hemicord and acting on the intact reticulospinal fibres. In development, crossing the midline is regulated by an interplay of attractive and repellent factors (Evans and Bashaw, 2010). Not much is known about such factors in the adult and injured CNS (Omoto *et al*., 2011), and more detailed molecular studies are

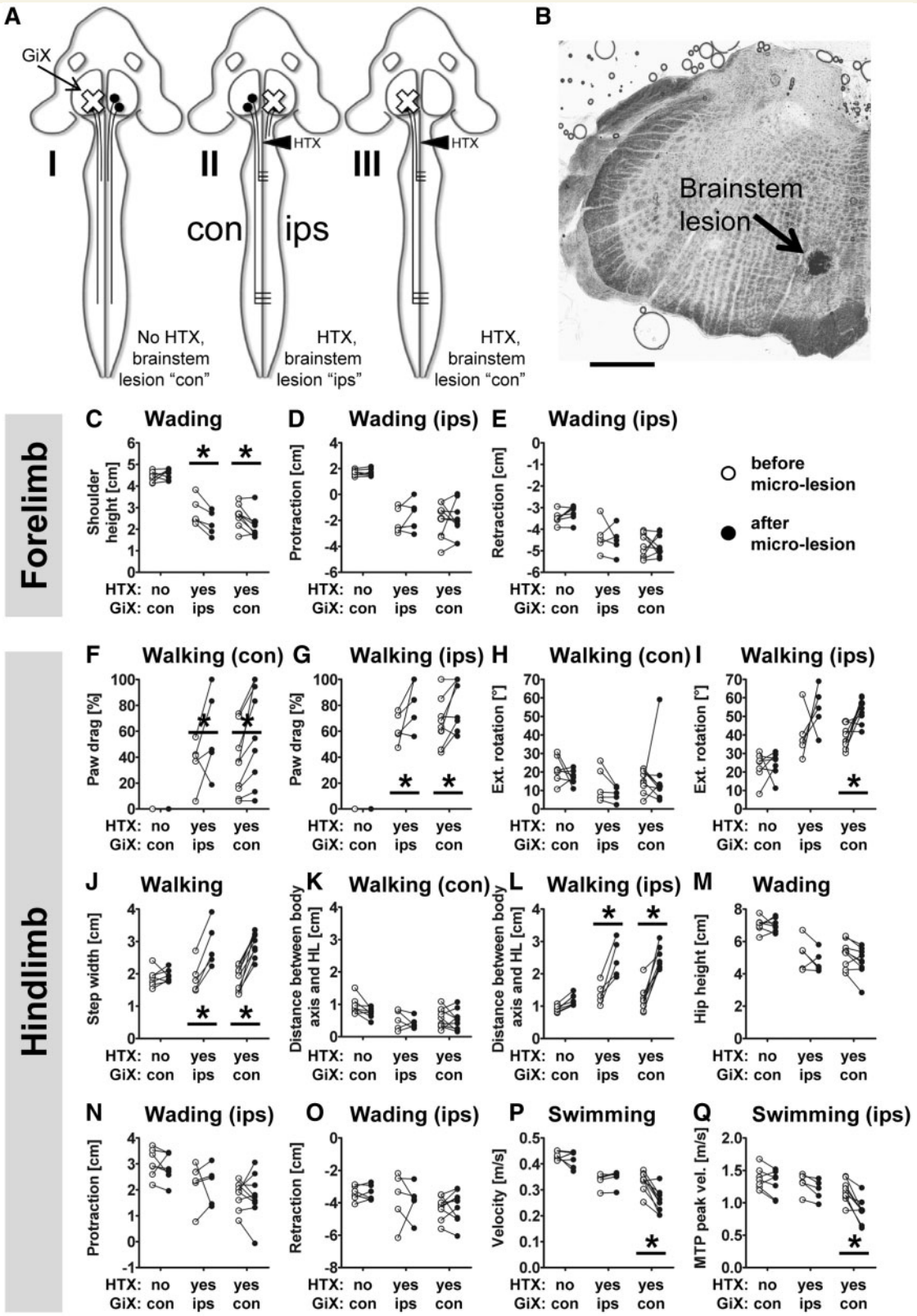

Figure 7 Lesioning of the gigantocellular reticular nucleus in recovered rats. (**A I–III**) Scheme illustrating the experimental approach. Intact rats received an electrolytic micro-lesion of the left gigantocellular reticular nucleus whereas rats that had recovered from hemisection injury for a period of 16 weeks received a lesion of the ipsilesional or the contralesional gigantocellular reticular nucleus. (**B**) Nissl staining demonstrating a representative electrolytic microlesion of the ventromedial portion of the contralesional gigantocellular reticular nucleus in an injured rat. Scale bar = 1 mm. (**C–Q**) Functional performance was assessed 1 day before (white dots) and 2 days after focal brainstem lesion (black dots) in intact rats ($n = 7$) and in rats with unilateral hemisection injury and either damage to the ipsilesional ($n = 5$; ips) or

(continued)

needed to reveal the molecular mechanisms underlying axonal midline crossing in the adult CNS. In the lumbar spinal cord, crossed reticulospinal fibres established a similar structural organization to pre-existing reticulospinal midline crossings in intact rats with an analogous degree of arborization and a preference for the ventral grey matter (Zemlan *et al*., 1984; Martin *et al*., 1985). Interestingly, in contrast with the lumbar cord there was a tendency towards a reduced arborization of the midline-crossing reticulospinal fibres in the ipsilesional cervical spinal grey matter. This anatomical finding correlates with function: the ipsilesional forelimb remained more impaired and recovered less than the ipsilesional hindlimb after the hemisection injury. The rat model is comparable with the situation in humans, but the mechanisms underlying these segmental differences in plasticity require further investigation.

Crossed reticulospinal neurons innervating new targets in the ipsilesional hemicord may face the problem of an inappropriate or even side-inverted input. After retrograde tracing from the gigantocellular reticular nucleus, we found labelled neurons widely-spread throughout the pontine and medullar reticular formation and, especially, in the contralateral counterpart of the traced gigantocellular reticular nucleus. In addition, the gigantocellular reticular nucleus received bilateral input from higher control centres in particular the MLR, as previously described (Steeves and Jordan, 1984; Garcia-Rill *et al*., 1986) and the rostral motor cortex (Antal, 1984; Matsuyama *et al*., 2004). Electrical stimulation experiments provided evidence that the MLR is capable of initiating basic locomotor behaviours in mammals (Shik *et al*., 1969; Ross and Sinnamon, 1984) via reticulospinal-interneuronal pathways controlling motor neuron pools of proximal and axial muscles (Noga *et al*., 2003; Matsuyama *et al*., 2004). Recent data in primates support the theory that the reticulospinal system is also important for the execution of precise finger and hand movements (Davidson and Buford, 2006; Alstermark and Isa, 2012), a task typically requiring the involvement of cortical premotor regions (Kaas *et al*., 2012). In rats, the rostral motor cortex accommodates primary motor neurons involved in controlling skilled forelimb movements (rostral forelimb area) but is also considered as a premotor region (Passingham *et al*., 1988; Rouiller *et al*., 1993). In the present study, hemisection injury was followed by poor recovery of fine motor control, and retrograde tracing revealed that the input from the rostral motor cortex to the gigantocellular reticular nuclei remained unchanged. In contrast, innervation of the contralesional gigantocellular reticular nucleus from the MLR (with a typically stronger ipsilateral input) changed to a more equal bilateral projection pattern, thus extending the influence of the ipsilesional MLR on the contralesional reticular nucleus (Fig. 8). We were not able to characterize these changes in more detail due to the limitations of retrograde tracing. As the measure of lateralization was a ratio and analysis of absolute cell counts was not useful because of high within-group variability, a higher lateralization index may be due to an increase in axons emanating from the ipsilesional MLR or to a reduction of projections from the contralesional MLR. Nevertheless, the balance of the MLRs' innervation pattern was modified in response to hemisection injury which may reflect the input adjustments needed by newly crossed reticulospinal neurons to convey purposeful information to their novel targets in the ipsilesional hemicord. Whether input modification occurred as a consequence of the midline crossing at spinal levels to provide crossed neurons with appropriate information ('bottom-up') or whether, in fact, the changed input from supraspinal control centres enforced the spinal adaptations ('top-down') remains to be elucidated.

Electrolytic microlesioning of the ventromedial portion of the gigantocellular reticular nucleus was performed to determine the functional relevance of the anatomical changes in rats recovered from hemisection injury. Intact rats did not show any behavioural deficits after unilateral destruction of the gigantocellular reticular nucleus and this was most likely due to compensation through other, spared descending CNS systems. In contrast, damage to either the ipsi- or contralesional gigantocellular reticular nucleus in behaviourally recovered, walking rats with chronic unilateral hemisection injury abolished the recovered behaviour. Interestingly, a lesion of the ipsilesional gigantocellular reticular nucleus that had lost all of its ipsilesionally descending projections below C4 led to similar devastating consequences during walking and wading as damage to the contralesional nucleus. Thus, the ipsilesional gigantocellular reticular nucleus may exert some influence on basic locomotor functions after hemisection either by way of reciprocal connections with its contralesional counterpart or through detour pathways including relay interneurons located in the cervical spinal cord above the lesion (Reed *et al*., 2006; Cowley *et al*., 2008). However, functional assessment during swimming demonstrated behavioural deficits of the ipsilesional hindlimb that were specific to the inactivation of the contralesional gigantocellular reticular nucleus. This confirms that the observed anatomical changes in the contralesional reticulospinal system made a substantial contribution to functional recovery after hemisection injury.

In conclusion, functionally-relevant anatomical plasticity, which can be as drastic as inducing a left-right side switch of axonal projection in the spinal cord and brainstem, can also occur in the oldest part of the CNS with its functionally basic neuronal circuits. A deeper knowledge of such elementary adaptations mediating spontaneous recovery after CNS damage is fundamental for the development of new therapeutic approaches aiming for improved recovery in humans (Lu *et al*., 2012).

Figure 7 Continued
contralesional ($n = 9$; con) gigantocellular reticular nucleus. Locomotor performance was assessed during walking, wading and swimming using similar parameters for the fore- (**C–E**) and hindlimbs (**F–Q**) as described for Fig. 1. Results are presented for each individual rat. For differences between time points (before and after brainstem lesion) and groups, repeated measures two-way ANOVA was performed followed by Bonferroni's Multiple Comparison Test with $*P < 0.05$ indicating significantly different results between time points.
HTX = hemisection; GiX = micro-lesion of the gigantocellular reticular nucleus; HL = hindlimb; MTP = metatarsophalangeal joint.

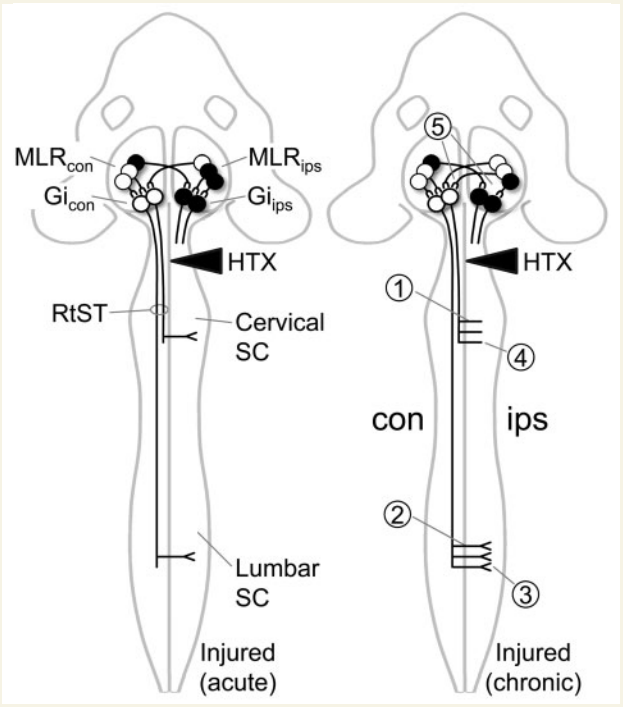

Figure 8 Summary of findings on anatomical plasticity in the reticular mesencephalic-medullar-spinal pathway after unilateral spinal cord injury in rats. The scheme shows the supraspinal connections between the MLR and the gigantocellular reticular nucleus (Gi) located in the medulla oblongata. In addition, spinal projections of the gigantocellular reticular nucleus running in the reticulospinal tract (RtST) are illustrated. An acute cervical unilateral hemisection injury (HTX) severs reticulospinal fibres that descend in the ipsilesional hemicord while contralesional axons are spared. Limited reticular innervation of the ipsilesional hemicord below the lesion site is provided by a few 'pre-existing' midline crossing reticulospinal axons. In rats that recovered from injury over a period of at least 4 weeks (chronic), projections within the reticular network are modified at the level of the brainstem and the spinal cord compared to the acute state. In these rats, more spared contralesional reticulospinal fibres cross the midline at cervical (1) and lumbar (2) spinal segments reaching the ipsilesional spinal cord grey matter below the injury site. In the chronic situation, fibres crossing the midline at lumbar levels demonstrate a degree of branching similar to that of 'pre-existing' reticulospinal midline crossing fibres in intact and, most likely, also in acutely injured rats (3). In contrast, fibres that cross the spinal cord midline at cervical segments show a lower degree of branching in the cervical grey matter (4). Changes of the spinal projection pattern of the contralesional gigantocellular reticular nucleus in recovered rats are accompanied by modifications of the nucleus' input. Normally, the gigantocellular reticular nucleus receives a stronger input from the ipsilateral than from the contralateral MLR (ratio of about 2:1). In rats that have recovered from hemisection injury, this relation is changed implicating a stronger influence of the ipsilesional MLR on the contralesional gigantocellular reticular nucleus (5).
MLR$_{con}$ = contralesional mesencephalic locomotor region; MLR$_{ips}$ = ipsilesional mesencephalic locomotor region; Gi$_{con}$ = contralesional gigantocellular reticular nucleus; Gi$_{ips}$ = ipsilesional gigantocellular reticular nucleus; con = contralesional; ips = ipsilesional; SC = spinal cord.

Funding

This study was supported by grants from the Swiss National Science Foundation (31-63633.00 and 3100AO-122527/1), the National Center for Competence in Research 'Neural Plasticity and Repair' of the Swiss National Science Foundation, the Spinal Consortium of the Christopher and Dana Reeve Foundation and the Framework Program 7 EU Collaborative Project Spinal Cord Repair.

Supplementary material

Supplementary material is available at *Brain* online.

References

Alstermark B, Isa T. Circuits for skilled reaching and grasping. Annu Rev Neurosci 2012; 35: 559–78.
Antal M. Termination areas of corticobulbar and corticospinal fibres in the rat. J Hirnforsch 1984; 25: 647–59.
Armstrong DM. The supraspinal control of mammalian locomotion. J Physiol 1988; 405: 1–37.
Ballermann M, Fouad K. Spontaneous locomotor recovery in spinal cord injured rats is accompanied by anatomical plasticity of reticulospinal fibers. Eur J Neurosci 2006; 23: 1988–96.
Bareyre FM, Kerschensteiner M, Raineteau O, Mettenleiter TC, Weinmann O, Schwab ME. The injured spinal cord spontaneously forms a new intraspinal circuit in adult rats. Nat Neurosci 2004; 7: 269–77.
Basso DM, Beattie MS, Bresnahan JC. Descending systems contributing to locomotor recovery after mild or moderate spinal cord injury in rats: experimental evidence and a review of literature. Restor Neurol Neurosci 2002; 20: 189–218.
Bertelli JA, Mira JC. Behavioral evaluating methods in the objective clinical assessment of motor function after experimental brachial plexus reconstruction in the rat. J Neurosci Methods 1993; 46: 203–8.
Courtine G, Gerasimenko Y, van den Brand R, Yew A, Musienko P, Zhong H, et al. Transformation of nonfunctional spinal circuits into functional states after the loss of brain input. Nat Neurosci 2009; 12: 1333–42.
Courtine G, Song B, Roy RR, Zhong H, Herrmann JE, Ao Y, et al. Recovery of supraspinal control of stepping via indirect propriospinal relay connections after spinal cord injury. Nat Med 2008; 14: 69–74.
Courtine G, van den Brand R, Musienko P. Spinal cord injury: time to move. Lancet 2011; 377: 1896–8.
Cowley KC, Zaporozhets E, Schmidt BJ. Propriospinal neurons are sufficient for bulbospinal transmission of the locomotor command signal in the neonatal rat spinal cord. J Physiol 2008; 586: 1623–35.
Dancause N, Barbay S, Frost SB, Plautz EJ, Chen D, Zoubina EV, et al. Extensive cortical rewiring after brain injury. J Neurosci 2005; 25: 10167–79.
Davidson AG, Buford JA. Bilateral actions of the reticulospinal tract on arm and shoulder muscles in the monkey: stimulus triggered averaging. Exp Brain Res 2006; 173: 25–39.
Evans TA, Bashaw GJ. Axon guidance at the midline: of mice and flies. Curr Opin Neurobiol 2010; 20: 79–85.
Filli L, Zorner B, Weinmann O, Schwab ME. Motor deficits and recovery in rats with unilateral spinal cord hemisection mimic the Brown-Sequard syndrome. Brain 2011; 134 (Pt 8): 2261–73.
Garcia-Rill E, Skinner RD, Conrad C, Mosley D, Campbell C. Projections of the mesencephalic locomotor region in the rat. Brain Res Bull 1986; 17: 33–40.

Gelderd JB, Chopin SF. The vertebral level of origin of spinal nerves in the rat. Anat Rec 1977; 188: 45–7.
Gensel JC, Tovar CA, Hamers FP, Deibert RJ, Beattie MS, Bresnahan JC. Behavioral and histological characterization of unilateral cervical spinal cord contusion injury in rats. J Neurotrauma 2006; 23: 36–54.
Ghosh A, Sydekum E, Haiss F, Peduzzi S, Zorner B, Schneider R, et al. Functional and anatomical reorganization of the sensory-motor cortex after incomplete spinal cord injury in adult rats. J Neurosci 2009; 29: 12210–9.
Goshgarian HG. The crossed phrenic phenomenon: a model for plasticity in the respiratory pathways following spinal cord injury. J Appl Physiol 2003; 94: 795–810.
Grillner S. Neural networks for vertebrate locomotion. Sci Am 1996; 274: 64–9.
Grillner S, Wallen P. Central pattern generators for locomotion, with special reference to vertebrates. Annu Rev Neurosci 1985; 8: 233–61.
Grillner S, Wallen P, Saitoh K, Kozlov A, Robertson B. Neural bases of goal-directed locomotion in vertebrates—an overview. Brain Res Rev 2008; 57: 2–12.
Hagglund M, Borgius L, Dougherty KJ, Kiehn O. Activation of groups of excitatory neurons in the mammalian spinal cord or hindbrain evokes locomotion. Nat Neurosci 2010; 13: 246–52.
Jankowska E, Stecina K, Cabaj A, Pettersson LG, Edgley SA. Neuronal relays in double crossed pathways between feline motor cortex and ipsilateral hindlimb motoneurones. J Physiol 2006; 575: 527–41.
Kaas JH, Stepniewska I, Gharbawie O. Cortical networks subserving upper limb movements in primates. Eur J Phys Rehabil Med 2012; 48: 299–306.
Kapitza S, Zorner B, Weinmann O, Bolliger M, Filli L, Dietz V, et al. Tail spasms in rat spinal cord injury: changes in interneuronal connectivity. Exp Neurol 2012; 236: 179–89.
Laouris Y, Kalli-Laouri J, Schwartze P. The postnatal development of the air-righting reaction in albino rats. Quantitative analysis of normal development and the effect of preventing neck-torso and torso-pelvis rotations. Behav Brain Res 1990; 37: 37–44.
Lindau NT, Banninger BJ, Gullo M, Good NA, Bachmann LC, Starkey ML, et al. Rewiring of the corticospinal tract in the adult rat after unilateral stroke and anti-Nogo-A therapy. Brain 2014; 137 (Pt 3): 739–56.
Little JW, Halar E. Temporal course of motor recovery after Brown-Sequard spinal cord injuries. Paraplegia 1985; 23: 39–46.
Lu P, Blesch A, Graham L, Wang Y, Samara R, Banos K, et al. Motor axonal regeneration after partial and complete spinal cord transection. J Neurosci 2012; 32: 8208–18.
Markham CH. Vestibular control of muscular tone and posture. Can J Neurol Sci 1987; 14 (3 Suppl): 493–6.
Martin GF, Vertes RP, Waltzer R. Spinal projections of the gigantocellular reticular formation in the rat. Evidence for projections from different areas to laminae I and II and lamina IX. Exp Brain Res 1985; 58: 154–62.
Matsuyama K, Mori F, Nakajima K, Drew T, Aoki M, Mori S. Locomotor role of the corticoreticular-reticulospinal-spinal interneuronal system. Prog Brain Res 2004; 143: 239–49.
McCrea DA, Rybak IA. Organization of mammalian locomotor rhythm and pattern generation. Brain Res Rev 2008; 57: 134–46.
Metz GA, Whishaw IQ. Cortical and subcortical lesions impair skilled walking in the ladder rung walking test: a new task to evaluate fore- and hindlimb stepping, placing, and co-ordination. J Neurosci Methods 2002; 115: 169–79.
Noga BR, Kriellaars DJ, Brownstone RM, Jordan LM. Mechanism for activation of locomotor centers in the spinal cord by stimulation of the mesencephalic locomotor region. J Neurophysiol 2003; 90: 1464–78.
Nudo RJ. Mechanisms for recovery of motor function following cortical damage. Curr Opin Neurobiol 2006; 16: 638–44.
Omoto S, Ueno M, Mochio S, Yamashita T. Corticospinal tract fibers cross the ephrin-B3-negative part of the midline of the spinal cord after brain injury. Neurosci Res 2011; 69: 187–95.
Passingham RE, Myers C, Rawlins N, Lightfoot V, Fearn S. Premotor cortex in the rat. Behav Neurosci 1988; 102: 101–9.
Paxinos G, Watson C. The rat brain in stereotaxic coordinates. 4th edn. San Diego, CA, USA: Academic Press, Inc.; 1998.
Pellis SM, Pellis VC, Teitelbaum P. Air righting without the cervical righting reflex in adult rats. Behav Brain Res 1991; 45: 185–8.
Raineteau O, Schwab ME. Plasticity of motor systems after incomplete spinal cord injury. Nat Rev Neurosci 2001; 2: 263–73.
Raineteau O, Fouad K, Noth P, Thallmair M, Schwab ME. Functional switch between motor tracts in the presence of the mAb IN-1 in the adult rat. Proc Natl Acad Sci USA 2001; 98: 6929–34.
Reed WR, Shum-Siu A, Onifer SM, Magnuson DS. Inter-enlargement pathways in the ventrolateral funiculus of the adult rat spinal cord. Neuroscience 2006; 142: 1195–207.
Ross GS, Sinnamon HM. Forelimb and hindlimb stepping by the anesthetized rat elicited by electrical stimulation of the pons and medulla. Physiol Behav 1984; 33: 201–8.
Rossignol S, Frigon A. Recovery of locomotion after spinal cord injury: some facts and mechanisms. Annu Rev Neurosci 2011; 34: 413–40.
Rouiller EM, Moret V, Liang F. Comparison of the connectional properties of the two forelimb areas of the rat sensorimotor cortex: support for the presence of a premotor or supplementary motor cortical area. Somatosens Mot Res 1993; 10: 269–89.
Ryczko D, Dubuc R. The multifunctional mesencephalic locomotor region. Curr Pharm Des 2013; 19: 4448–70.
Sayad WY, Harvey SC. The regeneration of the Meninges: the dura mater. Ann Surg 1923; 77: 129–41.
Shik ML, Severin FV, Orlovsky GN. Control of walking and running by means of electrical stimulation of the mesencephalon. Electroencephalogr Clin Neurophysiol 1969; 26: 549.
Smith NJ, Horst NK, Liu B, Caetano MS, Laubach M. Reversible inactivation of rat premotor cortex impairs temporal preparation, but not inhibitory control, during simple reaction-time performance. Front Integr Neurosci 2010; 4: 124.
Starkey ML, Bleul C, Zorner B, Lindau NT, Mueggler T, Rudin M, et al. Back seat driving: hindlimb corticospinal neurons assume forelimb control following ischaemic stroke. Brain 2012; 135 (Pt 11): 3265–81.
Steeves JD, Jordan LM. Autoradiographic demonstration of the projections from the mesencephalic locomotor region. Brain Res 1984; 307: 263–76.
Webster DM, Steeves JD. Funicular organization of avian brainstem-spinal projections. J Comp Neurol 1991; 312: 467–76.
Weishaupt N, Hurd C, Wei DZ, Fouad K. Reticulospinal plasticity after cervical spinal cord injury in the rat involves withdrawal of projections below the injury. Exp Neurol 2013; 247C: 241–9.
Whishaw IQ, Gorny B, Sarna J. Paw and limb use in skilled and spontaneous reaching after pyramidal tract, red nucleus and combined lesions in the rat: behavioral and anatomical dissociations. Behav Brain Res 1998; 93: 167–83.
Zemlan FP, Behbehani MM, Beckstead RM. Ascending and descending projections from nucleus reticularis magnocellularis and nucleus reticularis gigantocellularis: an autoradiographic and horseradish peroxidase study in the rat. Brain Res 1984; 292: 207–20.
Zorner B, Schwab ME. Anti-Nogo on the go: from animal models to a clinical trial. Ann N Y Acad Sci 2010; 1198 (Suppl 1): E22–34.
Zorner B, Filli L, Starkey ML, Gonzenbach R, Kasper H, Rothlisberger M, et al. Profiling locomotor recovery: comprehensive quantification of impairments after CNS damage in rodents. Nat Methods 2010; 7: 701–8.